Proc. of the 32nd International Symposium on Shock Waves (ISSW32)
doi:10.3850/978-981-11-2730-4_0018-cd

Fast dynamic registration of ultra-disperse carbon particles upon detonation of energetic materials

Konstantin Ten, Alexey Kashkarov, Eduard Pruuel, Ivan Rubtsov, Vladimir Titov
Lavrentiev Institute of Hydrodynamics, 15 Lavrentiev av., Novosibirsk, 630090, Russia
Boris Tolochko
Institute of Solid State Chemistry and Mechanochemistry, 18 Kutateladze str, Novosibirsk, 630128, Russia
Dmitriy Petrov, Aleksandr Garmashev, Evgeniy Smirnov
Russian Federal Nuclear Center, All-Russian Research Institute of Technical Physics, 13 Vasilyeva str., Snezhinsk, 456770, Russia

Corresponding Author: kten276@gmail.com

Annotation.
The paper presents experimental data on the dynamic registration of the sizes of condensed carbon nanoparticles upon detonation of oxygen-deficient energetic materials (EMs). The nanoparticle sizes were restored after processing of the measured distributions of small-angle X-ray scattering (SAXS). The work was carried out on the VEPP 3-4 accelerator complex (BINP SB RAS).

The dynamically measured dimensions of carbon nanoparticles are ~ 2–4 nm near the chemical reaction zone (CRZ). The size of carbon nanoparticles is maximum beyond the chemical reaction zone and is ~ 5-8 nm in TNT/RDX mixtures, and ~ 70 nm in BTF. With increase in the charge diameters from 20 mm to 40 mm (and the charge mass from 20 g to 200 g), the sizes of condensed nanoparticles grow by 15–20%.

Keywords. Detonation, oxygen-deficient energetic materials (EMs), carbon condensation, detonation nanodiamond, synchrotron radiation, small-angle X-ray scattering (SAXS)

1. Introduction.

Detonation processes in condensed EMs last less than 1 μs. For this reason, they should be studied using dynamic techniques with nanosecond exposures. This is especially true of carbon condensation processes upon detonation of oxygen-deficient EMs. Such work started at LIH in 1983 in connection with the activity on the synthesis of detonation nanodiamonds. These works have been actively continued at many scientific centers, and now there are more than 900 papers on this topic in the world [1]. The weight of EM charges under study ranged from 200 g to hundreds of kg, and their diameter was 40 mm and above. These works addressed mostly the remaining detonation products (chamber soot) collected after the explosion in the explosion chamber.

At that time, it was not possible to investigate experimentally the kinetics (dynamics) of carbon condensation. For this reason, it was taken that the place and time of condensation coincided with the chemical reaction zone because the medium parameters there corresponded to the steady phase of the diamond state [1, 2].

In the early 2000s, researchers in Novosibirsk started development of a new technique to study fast processes with the help of high-energy accelerators. The high intensity of synchrotron radiation (SR) enables recording of the dynamics of the SAXS distribution with an exposure of ~ 1 ns [3].

The SAXS intensity is proportional to the electron density fluctuations, which are associated with the carbon condensation upon detonation of EM. Model calculations have shown that it is possible to extract information on the size of carbon nanoparticles that are condensed in the chemical reaction zone, as well as outside it [3, 4], using the measured SAXS distributions. In the first works, the total SAXS was measured. Due to the development of the DIMEX detector, it became possible to measure the SAXS distribution and, therefore, the size dynamics of condensed nanoparticles. Dynamic measurements of SAXS were performed on the VEPP-3 collider at BINP SB RAS. The main feature of the VEPP-3 collider was a large current per bunch (~ 100 mA). The SR was produced by a single-pole shifter with a magnetic induction of 2T. The growth dynamics of condensed carbon nanoparticles in oxygen-deficient dense EMs (TNT, TNT/RDX alloys, TATB, and BTF) was measured at this setup. The results exhibited prolonged growth of the SAXS signals (~ 2-3 μs), whereas the chemical reaction zone of these EMs was ~ 0.1–1 μs [3 - 7]. The SAXS magnitude is linked with the size of condensed carbon, which poses a question: where is the end of the growth of nanodiamonds upon detonation of EM? The main drawbacks of these studies were the low level of SAXS signal and the low pulse repetition rate of SR pulses (~ 125 ns). These limitations are caused by the capabilities of the VEPP-3 collider.

Later, researchers at APS addressed the dynamic registration of SAXS at detonation of DNS and composition B [8, 9]. In these works, the EM charges were very small (diameter ~ 6 mm), and the growth of nanodiamond sizes stopped in 0.6 μs

In 2016, a new installation **SYRAFEEMA** (**Sy**nchrotron **Ra**diation **F**acility for **E**xploring **E**nergetic **M**aterials) was commissioned at BINP on the basis of the VEPP-4 collider [10]. VEPP-4 has an energy of 4.5 GeV, pulse length of ~ 100 ps, and repetition rate of up to 124 ns. SR pulses are produced by a 9-pole wiggler with a magnetic induction of 1.9 T. With this setup, the SAXS measurement technique enables recording of the dynamics of nanoparticles ranging from 4 to 200 nm in size.

This paper presents experimental data on the dynamics of carbon condensation on the **SYRAFEEMA** installation in TNT/RDX mixtures, as well as in a non-hydrogen EM of benzotrifuroxane (BTF). A characteristic feature of these experiments is the increased geometrical dimensions (diameter of up to 40 mm and weight of up to 200 g) of all explosive charges under investigation. In earlier works, the charge mass did not exceed 20 g. In the literature, there are data only for large charges [1, 2].

2. Experimental set-up

The research was carried out at the station to study the extreme state of matter on the VEPP-4 storage ring [10]. The signal scattered from nanoparticles was recorded with the DIMEX-3 detector [11, 12]. During the experiments, the SR beam was at a distance of ~ 15 mm from the upper end of the EM charge.

VEPP-4 (energy 4.5 GeV) was operated in the two-bunch regime with a current of 10 mA per bunch and a period of 600 ns. The SR pulse duration was ~ 100 ps [13]. In the explosion chamber, the entrance window and the exit windows were of beryllium 2 mm thick. The experiments were carried out at the atmospheric pressure in the explosion chamber.

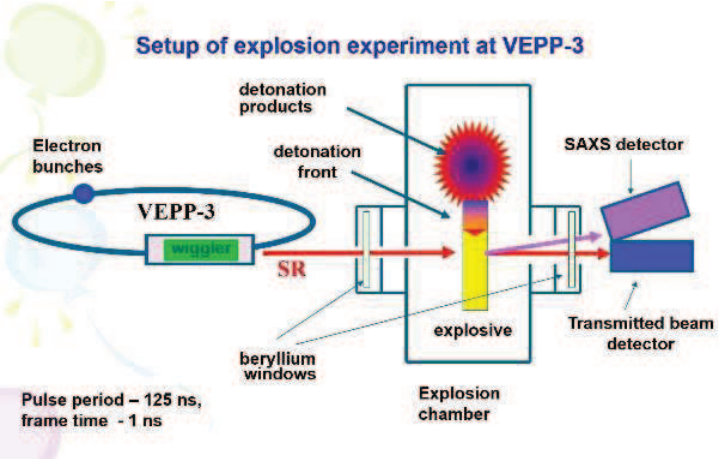

Fig.1. Experimental setup.

The distance from the axis of the explosive charge to the detector at the station on VEPP-4 was L_2 = 3432 mm; the interval between the channels (strips) of the DIMEX detector was 0.1 mm. That is, in these experiments on VEPP-4, one channel of the DIMEX detector corresponded to 0.02914 mrad (Fig. 1). In 1 ns, the detector recorded 512 channels (in fact, only the first 120 channels had a signal), which made up 1 frame. The distribution of SAXS from next bunch was recorded in next frame. In total, the detector was able to record 100 frames.

In our experiments, the minimum registration angles were 5 channels, $2\theta_{min} = 0.15$ mrad (where θ is the half scattering angle), and the maximum angle was 120 channels, $2\theta_{max} = 3.5$ mrad. In this case, the limit sizes of the recorded nanoparticles are determined by the following formulas [14]:

$$D_{min} = \frac{\pi}{q_{max}} = \frac{\lambda_{min}}{4 \cdot Sin(\theta_{max})} = 4nm$$

$$D_{max} = \frac{\pi}{q_{min}} = \frac{\lambda_{max}}{4 \cdot Sin(\theta_{min})} = 240nm$$

Here q - the scatter vector $q = \frac{4\pi}{\lambda} Sin\theta$.

Cast charges of trinitrotoluene (TNT) and its mixtures with hexogen (RDX) with diameters of 20 mm, 30 mm, and 40 mm were investigated (Fig. 2). The length of the charges ranged from 55 mm to 65 mm; the charge density ρ = 1.65 g/cm^3.

Fig.2. Assembly with TNT/RDX charge of 40 mm in diameter.

3. Experimental results.

The SAXS recording channel was tuned using a dummy with nanodiamonds (ultra-disperse explosion nanodiamonds (UDDs) of 4-6 nm in size). The dummy with nanodiamonds was put at the place of the EM charge to study, the main SR beam closed by blades for the SAXS signal from the UDD to be15 times greater than that from the air in the explosion chamber.

Fig. 3 shows records of the SAXS variation upon detonation of TNT charges with a diameter of 30 mm. The X axis presents the angle of scattering in mrad. Different colors display successive distributions of SAXS (frames) with step of 0.6 μs. The blue curve corresponds to the passage of the detonation front through the plane of the SR beam. Fig. 4 shows records of the SAXS variation upon detonation of TG50/50 charges with a diameter of 40 mm. The step between frames – 1.2 μs.

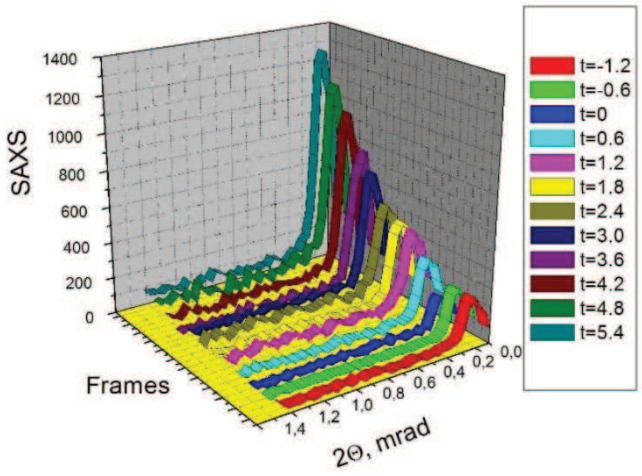

Fig. 3. SAXS distribution variation upon detonation of TNT charge of 30 mm in diameter. Different colors display SAXS distributions (Frames) with step of 0.6 μs.

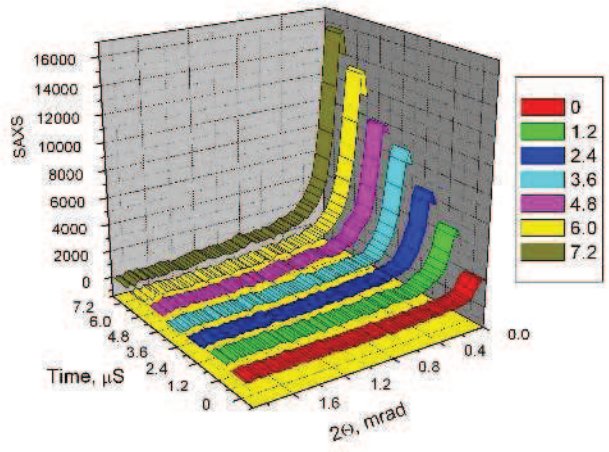

Fig. 4. SAXS variation upon detonation of TG50/50 charge of 40 mm in diameter. X axis: angle of scattering, mrad. Different colors display SAXS distributions with step of 1.2 μs.

4. Processing experimental data

Unlike earlier works [6–8, 13] and others, this paper takes into account the spread of the detonation products (for correct allowance of how the absorption affects the SAXS amplitude). The scattering of the products was calculated using the ANSYS Autodyn program for a Composition B (TG 40/60) charge of initial density of 1.72 g/cm^3, with the JWL equation of state in cylindrical symmetry. The calculations yielded the density distribution at different points in time. The distributions obtained were integrated over the radius, and **ρd** (mass on the beam) was computed at different points in time. For each frame, a particular ρd value was taken, using which the real radiation spectrum at the station and its effective energy were restored. Features of the calculation of real spectrum, as well as its replacement with the effective energy, are presented in [15, 16].

To obtain an acceptable signal level, we recorded white X-rays from the 9-pole wiggler. In [3, 5, 16], it was shown that radiation from this wiggler and the DIMEX detector used as a receiver enabled restoration of the average size of scattering nanoparticles. In this work, two techniques are used to restore the size of scattering nanoparticles. The Guinier method [14] was used to determine the dynamics of the average size of scattering nanoparticles. In the second method, SMD, the SAXS signal was approximated using a set of scattering intensities from homogeneous spherical particles of different diameters. Both methods give consistent results.

5.1. Guinier approximation

The sizes of the scattering centers can be restored in the Guinier approximation [14-Feigin]. In the approximation of small scattering angles, the intensity $I(q; R_g) \sim \exp(-q^2R^2/5)$, where R is the radius of spherical particle. Taking the logarithm of intensity $\ln(I(q; R)) = \ln(I_0) - q^2R^2/5$, we obtain a linearly decreasing function of q^2, from the slope of which k we can restore the spherical particle size D.

5.2. SMD method.

Assuming that photons with different energies do not interact with each other and each energy makes its own contribution to the total intensity, we approximated the experimental SAXS signal using a set of intensities from spherical particles of different sizes (1 to 200 nm) with different coefficients. These coefficients were selected to minimize the square of the sum of the differences between the experimental and calculated signals. The obtained coefficients gave the size distribution of the scattering nanoparticles .

The feasibility of these techniques in case of dynamic experiments was tested in static experiments on scattering from UDDs. According to analysis, the distributions of SAXS from UDDs in the Guinier approximation correspond to the particle size D = 6.2 nm (Fig. 5). The **SMD** method gives particle size distribution (Fig.6) with an average size of 6.3 nm [16].

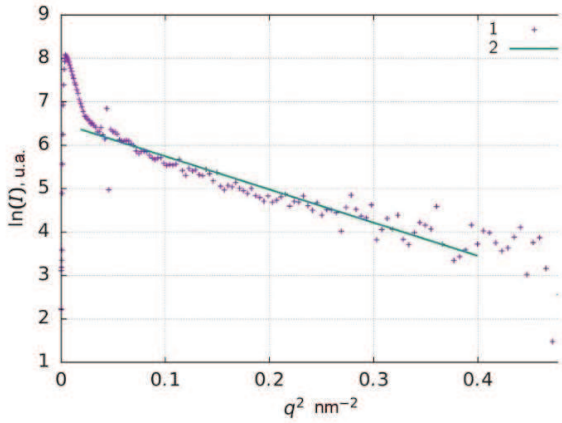

Fig. 5. ln(I) vs. q^2: 1 – ln(I), 2 – straight-line approximation for UDDs (k ≈ -7.7, D ≈ 6.2 nm). Exposure time: 100 ps.

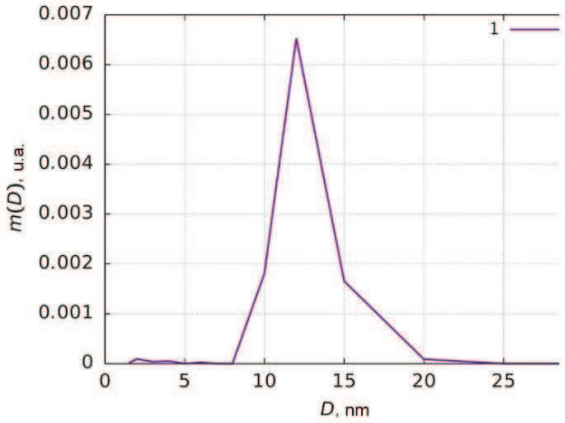

Fig. 6. Particle size distribution for UDDs for SMD. Average size: 6.3 nm.

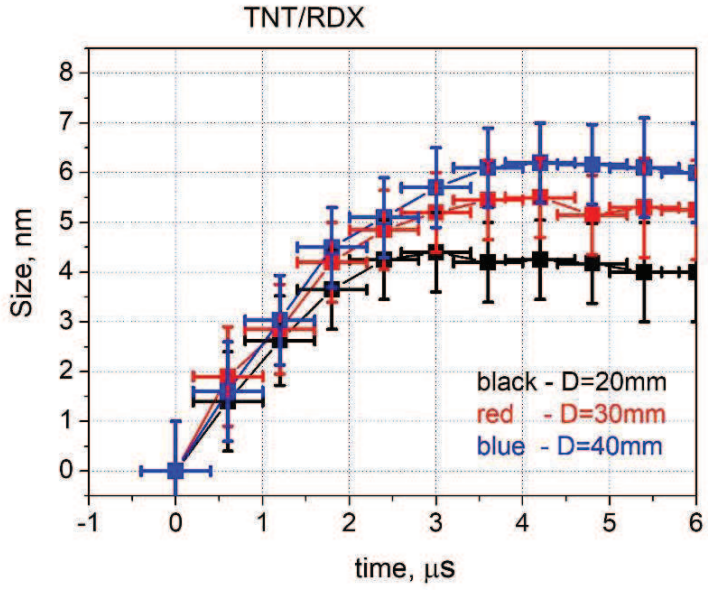

Fig. 7. Dynamics of average size of carbon nanoparticles upon detonation of TG50/50 charge of 20, 30, and 40 mm in diameter.

In the case of TNT/RDX charges, the experimental data obtained (Fig. 7) imply a long growth time (condensation) of carbon nanoparticles. With increase in the charge size, the condensation time grows weakly (by 10%); the maximum size of nanoparticles also increases (by 10-15%).

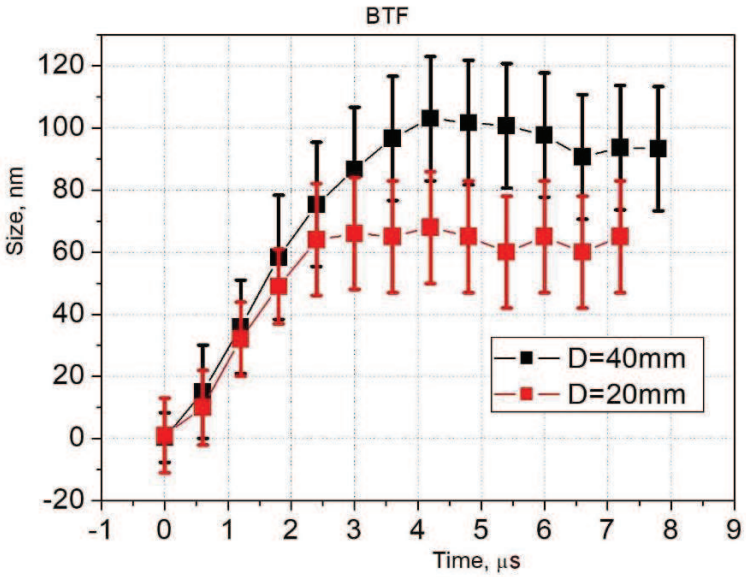

Fig. 8. Dynamics of growth of condensed carbon nanoparticles upon detonation of BTF.

In the case of BTF, an increase in the maximum size of nanoparticles is also observed with an increase in the diameter of the charges (fig.8).

6. Discussion of results.

When we first applied the method of SAXS measurement with high temporal resolution [that was round 2000], we were very surprised to see the SAXS growth within 2-3 μs. All works on the theory of detonation, as well as on the synthesis of nanodiamonds upon detonation of TG, asserted that all processes must end within the CRZ. Tarver [17] introduced the concept of two zones (regions) of carbon condensation, or divided the zone into two parts: fast (about 100 ns) and long (about 0.5 μs). The first part almost coincides with the chemical reaction zone (about 1 mm (at a detonation rate of 7.5 km/s, it is 130 ns)). The second part is much longer than the CRZ for TATB. The additional energy release in this zone made it possible to correctly describe experiments on the acceleration of strikers using TATB. An attempt to leave the CRZ for energy release was unusual (revolutionary) for those times. That might be the reason for taking a value of 0.5 μs (or 4 mm) behind the CRZ. More accurate measurements of velocities of strikers driven by long TATB charges revealed the dependence of the velocity on the charge length. To explain these results, an infinite carbon condensation time upon detonation of TATB was suggested in [18], or the border of the second zone shifted from 0.5 μs to infinity.

Conclusion.

Two carbon condensation zones are observed upon detonation of TNT/RDX charges. In the first (fast) one, regardless of the charge diameter, particles with a size of 4-6 nm are formed in less than 1 μs. The duration of the second zone depends on the charge diameter: it is approximately 3 μs for 20 mm and approximately 6 μs for 40 mm. In this zone, less dense

carbon structures of ~10 nm in size arise. We were not able to obtain quantitative data on the dependence of the duration of the second zone on the charge diameter.
In BTF charges, there are also two carbon condensation zones. The increase in the condensation time with the charge diameter charges is about 15%.
The results obtained are in reasonable agreement with experimental data on the dynamics of carbon condensation [3, 4, 5].

Acknowledgements. This work was partially supported by the Russian Foundation for Basic Research (project No. 16-29-01050).

References

[1] V.V. Danilenko. Synthesizing and sintering of diamond by explosion. **(**Energoatomizdat, Moscow, 2003). 272 p.
[2] V.M. Titov, V.F. Anisichkin and I.Yu. Mal'kov. Synthesis of ultradispersed diamond in detonation waves. Combustion, Explosion, and Shock Waves. **25,** 3 (1989)
[3] V. M. Titov, E. R. Pruuel, K. A. Ten, et al. Experience of Using Synchrotron Radiation for Studying Detonation Processes. Combustion, Explosion, and Shock Waves. **47**, 6, (2011)
[4] E. R. Pruuel, K. A. Ten, B. P. Tolochko, et al. Implementation of the capability of synchrotron radiation in a study of detonation processes. // Doklady Physics. **58**, 1, 2013
[5] V.M. Titov, B.P. Tolochko, K.A. Ten, et al. Where and when are nanodiamonds formed under explosion? Diamond & Related Materials. **16**, 12, (2007)
[6] K. A. Ten, E. R. Pruuel, V. M. Titov. SAXS Measurement and Dynamics of Condensed Carbon Growth at Detonation of Condensed High Explosives**.** Fullerenes, Nanotubes, and Carbon Nanostructures. **20** (2012).
[7] V.M. Aulchenko, O.V. Evdokov, K.A. Ten, et al. Current status and further improvements of the detector for imaging of explosions**.** Nuclear Instruments and Methods. **603**, 1-2 (2009)
[8] M. Bagge-Hansen, L. Lauderbach, et al. Measurement of carbon condensates using small-angle x-ray scattering during detonation of the high explosive hexanitrostilbene. Journal of Applied Physics. **117**. 24 (2015)
[9] E.B. Watkins, K.A. Velizhanin, D.M. Dattelbaum, et al. Evolution of Carbon Clusters in the Detonation Products of the Triamino-Trinitro-Benzene (TATB)-Based Explosive PBX 9502. J. Phys. Chem. C, (2017) DOI: 10.1021/acs.jpcc.7b05637
[10] B.P Tolochko, A.V. Kosov, O.V. Evdokov, et al. The synchrotron radiation beamline 8-b at VEPP-4 collider for SAXS, WAXS and micro tomography investigation of fast processes at extreme condition of high temperature and pressure with nanosecond time resolution. Physics Procedia, **84.** (2016)
[11] V.M. Aulchenko, A.E. Bondar, V.N. Kudryavtsev, et al. GEM-based detectors for SR imaging and particle tracking. Journal of Instrumentation, **7**, 03 (2012)
[12] L.I Shekhtman, V.M. Aulchenko, et al. Upgrade of the Detector for Imaging of Explosions. Physics Procedia. **84**. (2016)
[13] E.B. Levichev. Status and perspetives of VEPP-4 complex. Physics of Particles and Nuclei Letters. **XIII**, 7 (2016)
[14] L.A. Feigin, D.I. Svergun. Structure Analysis by Small-Angle X-Ray and Neutron Scattering**.** (Plenum Press, NY, 1987). P.335.
[15] I.A. Rubtsov, K.A. Ten, E.R. Pruuel, et al. Synchrotron radiation method for study the dynamics of nanoparticle sizes in trinitrotoluene detonation. Physics Procedia. **84**. (2016)
[16] I.A. Rubtsov, K.A. Ten, E.R. Pruuel, et al. The growth of carbon nanoparticles during the detonation of trinitrotoluene. Journal of Physics: Conference Series. **754,** 5. (2016)

[17] C.M Tarver., J.W Kury., R.D. Breithaupt. Detonation waves in triaminotrinitrobenzene**.** J. Appl. Phys. **82**. 8 (1997)
[18] K.F.Grebenkin, M.V.Taranik, A.L. Zherebtsov. **Computer modeling of scale effects at geterogeneous HE detonation.** Pros. 13th Symposium (International) on Detonation, (Norfolk, USA, 2006)